Journal of Organometallic Chemistry, 295 (1985) 239–256
Elsevier Sequoia S.A., Lausanne – Printed in The Netherlands

^{195}Pt, ^{119}Sn AND ^{31}P NMR STUDIES OF ALKYL, ARYL AND ACYL TRICHLOROSTANNATE COMPLEXES OF PLATINUM(II). THE CRYSTAL STRUCTURE OF *trans*-[Pt(SnCl$_3$)(COC$_6$H$_5$)(PEt$_3$)$_2$]

ALBERTO ALBINATI*

Istituto di Chimica Farmaceutica dell'Università di Milano, Viale Abruzzi 42, I-20131 Milano (Italy)

URS VON GUNTEN, PAUL S. PREGOSIN* and HUBERT J. RUEGG

Laboratorium für Anorganische Chemie, ETH Zentrum Universitätstrasse 6, CH-8092 Zürich (Switzerland)

(Received May 9th, 1985)

Summary

^{195}Pt, ^{119}Sn and ^{31}P NMR characteristics of the complexes *trans*-[Pt(SnCl$_3$)(carbon ligand)(PEt$_3$)$_2$] (**1a**–**1e**) are reported, (carbon ligand = CH$_3$ (**1a**), CH$_2$Ph (**1b**), COPh (**1c**), C$_6$Cl$_5$ (**1d**), C$_6$H$_4$Y (**1e**); Y = *meta*- and *para*-NO$_2$, CF$_3$, Br, H, CH$_3$, OCH$_3$, or {Pt(SnCl$_3$)(PEt$_3$)$_2$}). The values of $^1J(^{195}$Pt, ^{119}Sn) vary from 2376 to 11895 Hz with the COPh ligand having the smallest and the C$_6$Cl$_5$ ligand the largest value, making a total range for this coupling constant, when the dimer *syn–trans*-[PtCl(SnCl$_3$)(PEt$_3$)]$_2$ is included, of ca. 33000 Hz. In the *meta*- and *para*-substituted phenyl complexes $^1J(^{195}$Pt, ^{119}Sn) (a) is greater for electron-withdrawing substituents, (b) varies more for the *meta*-substituted derivatives (5634 to 7906 Hz) than for the *para* analogues (6088 to 7644 Hz) and (c) has the lowest values when the {Pt(SnCl$_3$)(PEt$_3$)$_2$} group is the *meta*- or *para*-substituent. The direction of the change in $^1J(^{195}$Pt, ^{119}Sn) is opposite to that found for $^1J(^{195}$Pt, ^{31}P). For the aryl complexes linear correlations are observed between $\delta(^{119}$Sn), $^1J(^{195}$Pt, ^{119}Sn), $^1J(^{195}$Pt, ^{31}P), $^2J(^{119}$Sn, ^{31}P) and the Hammett substituent constant σ^n. $\delta(^{119}$Sn) and $^1J(^{195}$Pt, ^{119}Sn) are related linearly to ν(Pt–H) in the complexes *trans*-[PtH(C$_6$H$_4$Y)(PEt$_3$)$_2$]; $\delta(^{119}$Sn) and $\delta(^1$H) (hydride) are also linearly related. Based on $^1J(^{195}$Pt, ^{119}Sn), the acyl ligand is suggested to have a very large NMR *trans* influence. The differences in the NMR parameters for (**1a**–**e**) are rationalized in terms of differing σ- and π-bonding abilities of the carbon ligands.

The structure of **1c** has been determined by crystallographic methods. The complex has a slightly distorted square planar geometry with *trans*-PEt$_3$ ligands. Relevant bond lengths (Å) and bond angles (°) are: Pt–Sn, 2.634(1), Pt–P, 2.324(4) and 2.329(4), Pt–C, 2.05(1); P–Pt–P, 170.7(6), Sn–Pt–C, 173.0(3), Sn–Pt–P, 92.1(1), 91.7(1), P–Pt–C, 88.8(4) and 88.3(4). The Pt–Sn bond separation is the longest yet observed for square-planar platinum trichlorostannate complexes, and would be

0022-328X/85/$03.30

consistent with a large crystallographic *trans* influence of the benzoyl ligand. The Pt–Sn bond separation is shown to correlate with ${}^1J({}^{195}\mathrm{Pt}, {}^{119}\mathrm{Sn})$.

---

1. Introduction

One-bond NMR spin–spin coupling constants involving a transition metal are now recognized as valuable analytical tools in complex chemistry [1,2]. In our studies on the coordination of the $SnCl_3$ ligand to platinum(II) [3–5] we have observed ${}^1J({}^{195}\mathrm{Pt}, {}^{119}\mathrm{Sn})$ coupling constants with magnitudes between 9 and 36 KHz, and have recently demonstrated a connection between this parameter and the Pt–Sn bond length [4]. Since we did not feel that the lower limit on ${}^1J({}^{195}\mathrm{Pt}, {}^{119}\mathrm{Sn})$ had been attained, we prepared the complexes *trans*-[Pt($SnCl_3$)(carbon ligand)(PEt_3)$_2$] (**1**) with the carbon ligands shown below. This selection of anionic carbon ligands contains CH_3 (**1a**), CH_2Ph (**1b**), COPh (**1c**), C_6Cl_5 (**1d**), *meta*- or *para*-substituted C_6H_4Y (**1e**), Y = NO_2, CF_3, Br, H, CH_3, OCH_3) potential π-acceptors as well as stronger and weaker σ-donors, and should allow us to explore ${}^1J({}^{195}\mathrm{Pt}, {}^{119}\mathrm{Sn})$ in further depth. Moreover, once the various ^{195}Pt, ^{119}Sn and ^{31}P NMR parameters for (**1a**–**1e**) have been evaluated we can use them as probes to estimate the relative donor capacities of these carbon ligands. We report here multinuclear NMR studies on the complexes **1**, the molecular structure of **1c**, and a relatively large NMR *trans* influence for the benzoyl ligand.

2. Results

(a) Preparation and characterization

The complexes **1** may be prepared by addition of anhydrous $SnCl_2$ to a solution containing *trans*-[PtCl(carbon ligand)(PEt_3)$_2$]. The novel bimetallated aryl complexes **2** and **3** were obtained as shown in eq. 1–3.

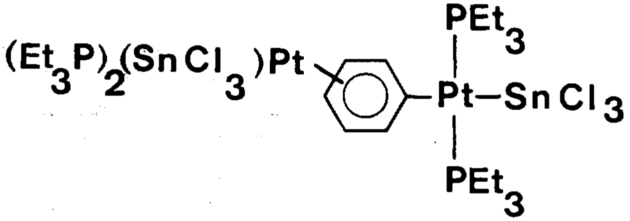

(**2** = *meta*-isomer;
3 = *para*-isomer)

$$2\,\mathrm{Pt(PEt_3)_3} + \textit{meta-}\text{ or }\textit{para-}\mathrm{BrC_6H_4Br} \xrightarrow[\text{Toluene}]{} \underset{(\mathbf{4}\text{ or }\mathbf{5})}{[(\mathrm{PEt_3})_2\mathrm{BrPtC_6H_4PtBr(PEt_3)_2}]} \quad (1)$$

$$\mathbf{4}\text{ or }\mathbf{5} \xrightarrow[\text{MeOH}]{+\mathrm{AgBF_4},\ \mathrm{LiCl}} \underset{(\mathbf{6}\text{ or }\mathbf{7})}{[(\mathrm{PEt_3})_2\mathrm{ClPtC_6H_4PtCl(PEt_3)_2}]} \quad (2)$$

$$\mathbf{6}\text{ or }\mathbf{7} + \text{xs }\mathrm{SnCl_2} \rightarrow \mathbf{2}\text{ or }\mathbf{3} \quad (3)$$

The new trichlorostannate complexes were characterized by NMR spectroscopic and microanalytical methods.

The ^{195}Pt and ^{119}Sn spectra for **1**–**3** are consistent with directly bound $SnCl_3$ in that they both show $^1J(^{195}Pt, ^{119}Sn)$ coupling constants. Moreover, the spectra exhibit triplet splittings arising from coupling of ^{31}P to ^{195}Pt and ^{119}Sn *, so that the coordination of both phosphines is assured. For the complexes **1a** and **1b**, the ^{1}H NMR spectra confirm the presence of the CH_3 and CH_2Ph groups. The benzoyl ligand can be identified from its ν(CO) IR stretch [6] and its low field *C*OR carbon resonance [7].

(b) Coupling constants

NMR data for the new complexes and some model analogs are shown in Table 1, and typical ^{119}Sn and ^{195}Pt spectra are shown in Figs. 1 and 2.

The complex *trans*-$[Pt(SnCl_3)(COPh)(PEt_3)_2]$ is striking in that ^1J(Pt, Sn) is only 2376 Hz. Since the dimer *syn–trans*-$[PtCl(SnCl_3)(PEt_3)]_2$ has ^1J(Pt, Sn) 35309 Hz [8], the value of ^1J(Pt, Sn) for an $SnCl_3$ coordinated to platinum(II) has changed by 32933 Hz, a factor of ca. 15 in relative terms. Typically, ^1J(Pt, L) varies by a factor of four to five for a given oxidation state of platinum [9].

The ^1J(Pt, Sn) value for *trans*-$[Pt(SnCl_3)(C_6Cl_5)(PEt_3)_2]$, 11895 Hz, is the largest in this series and is comparable to that found for $[Pt(SnCl_3)(EtO_2CC{=}CHCO_2Et)(PPh_3)_2]$, 11512 Hz [10] but larger than that for $[PtH(SnCl_3)(PEt_3)_2]$, 9067 Hz [11]. The methyl, phenyl and benzyl analogs have ^1J(Pt, Sn) values of 6620, 6352 and 5775 Hz, respectively. The values for the bimetallic complexes **2** and **3** (5634 and 6088 Hz), are at the low end of the range (5634–7906 Hz) found for phenyl substituted complexes. The introduction of an electron-withdrawing group on the aryl ligand increases ^1J(Pt, Sn), and the reverse is true for electron-donating substituents. One can consider *trans*-$[Pt(SnCl_3)(C_6Cl_5)(PEt_3)_2]$ as an extreme example of this trend, although the specific effects of *ortho* substitution of ^1J(Pt, Sn) are unknown. Interestingly, based on ^1J(Pt, Sn) for **2** and **3** (i.e. a platinum complex fragment as a substituent) one would expect that these metal moieties would be electron donors.

The values ^1J(Pt, P) for all the compounds vary from 2290 to 2666 Hz. Once again the C_6Cl_5 and COPh ligands represent the extremes; however, in this case the acyl ligand is associated with the larger value. Changes in this one-bond coupling constant with aryl substitution are modest, ca. 5% based on the parent complex, with the electron donors giving the larger values. Therefore, for ^1J(Pt, P) the overall trend in the aryl complexes is opposite to that observed for ^1J(Pt, Sn).

Both the ^{119}Sn and ^{31}P spectra show the two-bond coupling constant ^2J(Sn, P) which falls in the range 224–275 Hz. This is in agreement with previous measurements [3] for *cis* orientation of these two spins. Although the range within the aryl substituted complexes is relatively small, 224–250 Hz, we note that electron-withdrawing groups are associated with the larger values of this parameter.

---

* The various coupling constants will subsequently be abbreviated, e.g. ^1J(Pt, Sn), without reference to the respective atomic masses.

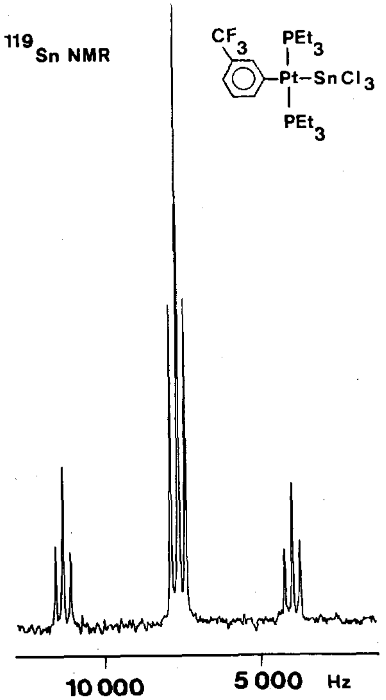

Fig. 1. ^{119}Sn{^{1}H} NMR spectrum of *trans*-[Pt(SnCl$_3$)(C$_6$H$_4$-*m*-CF$_3$)(PEt$_3$)$_2$], CD$_2$Cl$_2$, −60°C.

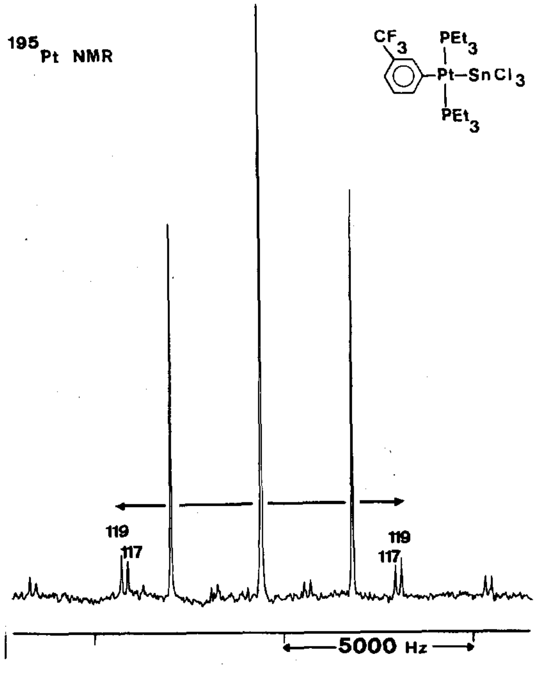

Fig. 2. ^{195}Pt{^{1}H} NMR spectrum of *trans*-[Pt(SnCl$_3$)(C$_6$H$_4$-*m*-CF$_3$)(PEt$_3$)$_2$], CD$_2$Cl$_2$, −60°C.

(c) Chemical shifts

The ^{119}Sn chemical shifts for the coordinated $SnCl_3$ ligands fall in the range -7 to $+140$ ppm relative to Me_4Sn. Normally, relatively high field absorptions are observed for $SnCl_3$ bound to platinum(II); e.g. $[PtCl_3(SnCl_3)]^{2-}$ has δ -596 ppm, and the dimer *syn–trans*-$[PtCl(SnCl_3)(PEt_3)]_2$ has δ -383 [8] indeed low field resonances, as in **1a**, are rare. We note that δ(^{119}Sn) for the methyl complex **1a** is similar to that for *trans*-$[PtH(SnCl_3)(PEt_3)_2]$, $+161$ ppm [11]. In any case, the total range for the $PtSnCl_3$ moiety is > 750 ppm, and is suggestive of very different Pt–Sn bonding characteristics at the two extremes. The aryl complexes afford ^{119}Sn signals in the range δ 75–99 ppm, with the electron-donor substituents producing low field chemical shifts. In contrast to the ^1J(Pt, Sn) data, the δ(^{119}Sn) data for the bimetallic complexes are not suggestive of any special electron-donating capability for the metal moiety, $\{Pt(SnCl_3)(PEt_3)_2\}$.

The ^{195}Pt chemical shifts fall at δ -4532 to -5003 ppm. In view of the known [12] sensitivity of δ(^{195}Pt) to changes within the coordination sphere of the metal, this is a modest, but significant change in this parameter. The resonance of the metal is not especially sensitive to the nature of the aryl substituent, δ -4800 to -4894 ppm (exclusion of the bimetallic complexes reduces this range to 68 ppm) suggesting, as do the ^{119}Sn chemical shift data, that the major electronic changes arise from change in the carbon ligand and not the aryl substitution pattern. The ^{31}P chemical shifts are found at δ 2.8–13.2 ppm with the C_6Cl_5 and CH_3 groups at the extremes. The effect of aryl substituent is small, < 3 ppm, with the donor groups shifting the phosphorus signal to lower field.

(d) Correlations involving the NMR parameters

In view of the sensitivity of several of our NMR parameters to the aryl substitution pattern we plotted δ(^{119}Sn), ^1J(Pt, Sn), ^1J(Pt, P) and ^2J(Sn, P) against the normal Hammett substituent constants, and found linear correlations in all

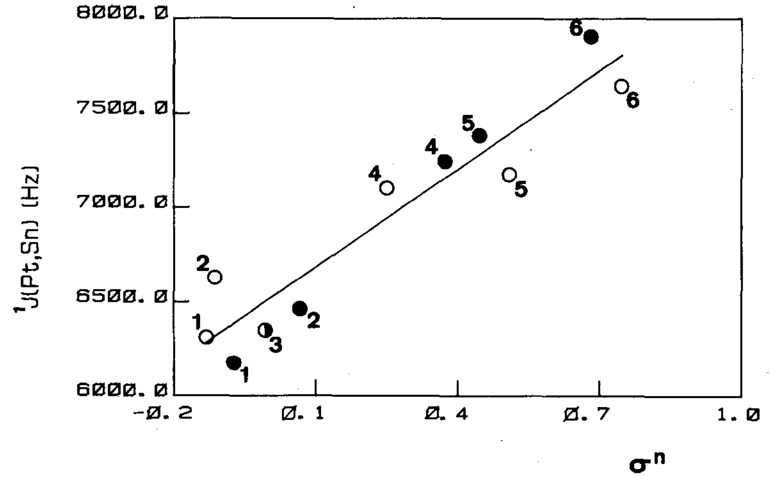

Fig. 3. Plot of ^1J(Pt, Sn) vs. the Hammett substituent constant, σ^n for the complexes *trans*-$[Pt(SnCl_3)(C_6H_4Y)(PEt_3)_2]$. Solid circles refer to *meta*- and open circles to *para*-substituents.

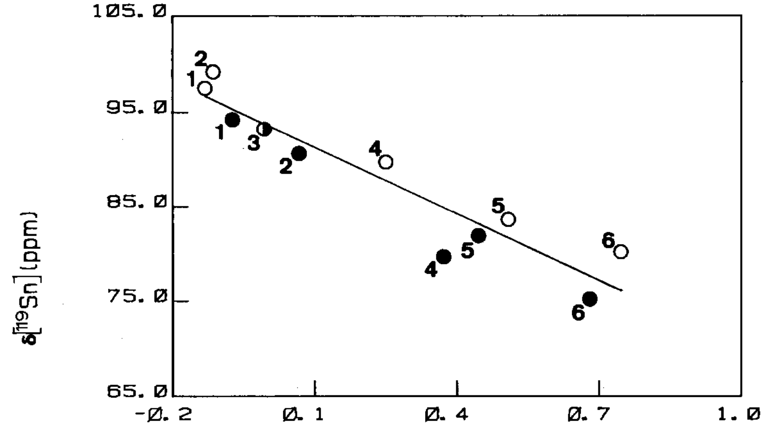

Fig. 4. Plot of $\delta(^{119}\mathrm{Sn})$ vs. the Hammett substituent constant, σ'' for the complexes *trans*-$[\mathrm{Pt(SnCl_3)(C_6H_4Y)(PEt_3)_2}]$. Solid circles refer to *meta*- and open circles to *para*-substituents.

cases. Examples of these correlations are shown in Fig. 3 and 4. The correlation coefficients for the two representations are 0.943 ($\delta(^{119}\mathrm{Sn})$ vs. σ'') and 0.947 (^1J(Pt, Sn) vs. σ''); however, we note that the coefficients for the lines arising from the *meta* analogues alone (0.983 and 0.999, respectively) are always larger than when the *meta* and *para* series are combined. Not surprisingly, there are a number of internal correlations, e.g., ^1J(Pt, Sn) correlates inversely with ^1J(Pt, P). This particular relationship is interesting in that there are known platinum(II) complexes where the *cis* and *trans* influences, as expressed by coupling constants, show similar inverse trends, e.g. between the two different ^1J(Pt, P) values in *cis*-$[\mathrm{PtCl(SnX_3)(PPh_3)_2}]$ [13] and $[\mathrm{Pt(carbon\ ligand)(PPh_3)_3}]\mathrm{BF_4}$ [14].

3. Discussion

It is customary to discuss the values ^nJ(M, L) and δ(M) (or δ(L)) in terms of the Fermi [15] and Ramsay [16] expressions, respectively (see eqs. 4 and 5).

$$^1J_{AB} \propto \gamma_A\gamma_B\,|\psi_{S,A}(0)|^2\,|\psi_{S,B}(0)|^2 \sum_i^{\mathrm{occ}} \sum_j^{\mathrm{unocc}} \left(^3\Delta E_{ij}\right)^{-1} C_{i,A}C_{j,A}C_{i,B}C_{j,B} \tag{4}$$

$$\sigma_A^P \propto (1/r^3) \sum_i^{\mathrm{occ}} \sum_j^{\mathrm{unocc}} \left(\Delta E_{ij}\right)^{-1} P \tag{5}$$

P = a sum involving the LCAO coefficients $C_{i,A}$ and $C_{j,A}$, for the x, y and z directions.

Consequently, for one-bond coupling constants and chemical shifts it is expected that changes in both the C-coefficients and energies of the complex molecular orbitals will determine the coupling constants and chemical shifts. In practice, the complexity of these molecules prohibits exact knowledge of these orbital energies

TABLE 1

NMR DATA[a] FOR THE Pt COMPLEXES

Compound	δ(Sn)	^1J(Pt, Sn)	^2J(Sn, P)	δ(Pt)	^1J(Pt, P)	δ(P)
1a[b]	140	6620	242	-5003	2452	13.2
1b	98	5775	258	-4945	2561	11.4
1c	87	2376	275	-4532	2666	6.1
1d[c]	-7.3	11895	273		2290	2.8
1e						
p-NO$_2$	80.2	7644	250	-4800[d]	2365	7.1
p-CF$_3$	83.6	7177	250	-4832[d]	2406	7.8
p-Br	89.7	7105	240	-4844	2413	8.5
p-H	93.3	6352	236	-4857[d]	2463	9.2
p-OCH$_3$	99.2	6629	233	-4862[d]	2453	10.0
p-CH$_3$	97.5	6314	234	-4864[d]	2471	9.5
m-NO$_2$	75.2	7906	248	-4829	2359	7.9
m-CF$_3$	81.9	7384	244	-4844	2394	8.5
m-Br	79.7	7247	243	-4851	2405	8.4
m-OCH$_3$	90.6	6464	237	-4856	2456	9.0
m-CH$_3$	94.2	6177	234	-4868	2477	9.3
2[e]	78.7	5634	247	-4885	2491	8.5
3[e]	89.5	6088	224	-4894	2474	8.1

[a] CD_2Cl_2 solution at -60°C, unless otherwise specified 0.02–0.03 *M*. Sn, Pt and P chemical shifts are relative to external Me_4Sn, K_2PtCl_6(aq) and H_3PO_4, respectively. Negative values indicate a signal at higher field than the reference. [b] -100°C, CD_2Cl_2. [c] 25°C, $CDCl_3$. [d] -10°C, CH_2Cl_2/C_6D_6, 4/1. [e] -86°C, CD_2Cl_2.

and coefficients, and so we chose to interpret our data using accepted empirical parameters together with model compounds from the literature.

Within this framework we address the following questions: (a) How large are the *cis* and *trans* influences of the $SnCl_3$ ligand? (b) How do the various carbon ligands differ as donors to platinum? (c) How important is π-bonding for the $SnCl_3$ and carbon ligands in the complexes?

(a) *cis and trans influences*

An evaluation of the ^{119}Sn and ^{31}P coupling constant data involves the *cis* and *trans* influence concepts [17], since the ^{119}Sn data vary as a function of the *trans* ligand and the ^{31}P data (Table 3) are dependent on the nature of the *cis* ligand. The NMR *trans* influence with respect to changes in coupling constants has been studied by various authors [18,19], and a strong *trans* influence is assigned to a ligand which brings about a marked decrease in the *trans* spin–spin coupling. For ^1J(Pt, H) [20], ^2J(Pt, H) [18], ^1J(Pt, P) [21], ^1J(Pt, C) [22] and ^1J(Pt, N) [23], the qualitative sequence is: anionic carbon ligand > tertiary phosphine > olefin > halogen. The *trans* influence for the $SnCl_3$ ligand may be estimated using *trans*-[Pt($SnCl_3$)(CH_3)(PEt_3)$_2$] and its ^2J(Pt, CH_3) value, since this two-bond coupling constant has been investigated extensively [18]. The observed value of 75.9 Hz suggests a moderate *trans* influence for the $SnCl_3$ ligand, not unlike that of an olefin [18]. This conclusion is in agreement with the results from crystallographic studies [24] using the Pt–Cl bond separation as a probe.

Interestingly, the $SnCl_3$ ligand is also associated with a significant *cis*-influence, which can be assessed by studying ^1J(Pt, P). Transformation of the complexes

TABLE 2

^1J(Pt, P) VALUES AND THE *cis* INFLUENCE FOR *trans*-[PtCl(X)(PEt$_3$)$_2$]

trans-[PtCl(X)(PEt$_3$)$_2$] X	^1J(Pt, P) (Hz)	Ref.
COPh	3003	this work
CH_3	2821	this work
CH_2Ph	2826	this work
Ph	2793	this work
H	2728	this work
C_6Cl_5	2609	26
C_2F_3	2510	25
C_6F_5	2486	27
Cl	2400	this work
PEt_3 [a]	2233	25
$SnCl_3$	2042	28
CO [b]	1830	25

[a] As ClO_4 salt. [b] As BF_4 salt.

trans-[PtCl(carbon ligand)(PEt$_3$)$_2$] to their SnCl$_3$ derivatives **1** is associated with a decrease in ^1J(Pt, P) of >300 Hz (see Tables 1 and 2). For the complexes *trans*-[PtX(C$_2$F$_3$)(PEt$_3$)$_2$] and *trans*-[PtL(C$_2$F$_3$)(PEt$_3$)$_2$]$^+$, Cairns et al. [25] find values for ^1J(Pt, P) from 2021 Hz to 2603 Hz with the smallest values found for L = a π-acceptor, e.g. when L = CO, ^1J(Pt, P) 2021 Hz; but for X = Cl, ^1J(Pt, P) 2510 Hz. Consequently, the SnCl$_3$ ligand appears to be a weak σ-donor and a potential π-acceptor. As shown in Table 2 ^1J(Pt, P) decreases in the order: COPh > CH$_3$ > Ph > C$_6$Cl$_5$ [26] > C$_6$F$_5$ [27] > Cl > SnCl$_3$ [28], where the last two entries in the sequence stem from *trans*-[PtCl$_2$(PEt$_3$)$_2$] and *trans*-[PtCl(SnCl$_3$)(PEt$_3$)$_2$].

(b) On the carbon ligand

The values ^1J(Pt, Sn) for our SnCl$_3$ complexes confirm that carbon ligands are indeed associated with a large *trans* influence, since these are amongst the smallest ^1J(Pt, Sn) values observed. Because of the five halogens, the C$_6$Cl$_5$ ligand is a weaker σ-donor than the C$_6$H$_5$ ligand, so that there is more *s*-character available for the SnCl$_3$ and therefore a larger ^1J(Pt, Sn) results. This view is also supported by a

TABLE 3

SOME ^{31}P NMR DATA [a] FOR THE COMPLEXES *trans*-[PtCl(C$_6$H$_4$-*p*-Y)(PEt$_3$)$_2$]

Y	^1J(Pt, P) (Hz)	$\delta(^{31}P)$
NMe_2	2796	14.6
OCH_3	2782	14.4
CH_3	2800	14.4
H	2793	14.3
Br	2743	13.9
CF_3	2732	11.9
NO_2	2690	13.7
NMe_2H^+	2722	14.2

[a] Room temperature in $CDCl_3$.

comparison of the ${}^{1}J$(Pt, H) values for *trans*-[PtH(C_6Cl_5)(PEt_3)$_2$], 729 Hz [26], and *trans*-[PtH(C_6H_5)(PEt_3)$_2$], 649 Hz [29]. Our observed ${}^{1}J$(Pt, Sn) values for the Ph and CH_3 compounds, i.e., 6352 and 6620 Hz, suggest the former carbon ligand exerts a larger *trans* influence than the latter, and once again this is in agreement with the hydride ${}^{1}H$ data, e.g. for *trans*-[PtHX(PPh_3)$_2$], X = Ph, CH_3, ${}^{1}J$(Pt, H) 600 and 656 Hz, respectively [30]. A smaller effect for CH_3 relative to CH_2Ph, based on the ${}^{1}J$(Pt, Sn) values of 6620 and 5775 Hz, respectively, is consistent with the observed ${}^{1}J$(Pt, P) values (*trans* to carbon) for [Pt(CH_3)(PPh_3)$_3$]BF_4, 1919 Hz and [Pt(CH_2Ph)(PPh_3)$_3$]BF_4 1795 Hz [14]. The very small ${}^{1}J$(Pt, Sn) value, 2376 Hz, for the benzoyl complex, **1c**, was not expected, and implies a large *trans* influence for this ligand. In support of this we can cite: (a) the relatively small ${}^{1}J$(Pt, P) value for the phosphorus ligand *trans* to carbon in **8**, when compared with phosphorus *trans* to CH_3 in **9**, and (b) the Pt–Cl bond length of 2.450(4) Å in *trans*-[PtCl($COPr^n$)(PPh_3)$_2$] [33], which is long when compared with the value of 2.408(5) Å found for *trans*-[PtCl(Ph)(PPh_3)$_2$] [34]. Consequently there is precedence for assigning the acyl ligand both a large NMR and a large crystallographic *trans* influence; however, the extent to which the benzoyl group has reduced ${}^{1}J$(Pt, Sn) is surprising, and this brings us to the theme of π-bonding.

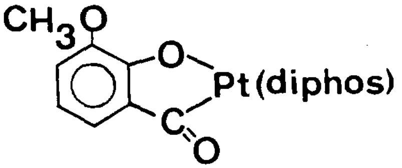

Pt(CH_3)(OC_6H_4-*p*-OCH_3)(diphos)

(8) ${}^{1}J$(Pt, P) 1496 Hz * [31] (*trans* to acyl)

(9) ${}^{1}J$(Pt, P) 1782 Hz [32] (*trans* to CH_3)

(c) π-bonding

Assumption of a $d\pi$–$d\pi$ interaction between platinum(II) and the $SnCl_3$ ligand would help us to account for the small value of ${}^{1}J$(Pt, Sn) in the benzoyl complex. If this carbon ligand functions as both σ-donor and π-acceptor, the *trans*-Pt–Sn bond will be relatively *s*-poor due to (a) the larger *s*-coefficient used in the Pt–C σ bond and (b) synergistic strengthening of the Pt–C bond as a consequence of the π-interaction. We sought support for this π-bonding hypothesis in terms of the ${}^{13}C$ chemical shift of the benzoyl carbon but, the δ value of 291.4 is reasonable [35] for an acyl ligand of this type without being informative. Interestingly, several authors have noted the rather short metal–acyl carbon separation observed in crystallographic studies [31,36,37], and one [36] has suggested this short distance to be the result of metal–carbon $d\pi$–$p\pi$ back bonding, so that our suggestion regarding the benzoyl complex is reasonable, if unproven.

A similar π-bonding rationale can be employed in discussing the ${}^{1}J$(Pt, Sn) results for the Ph and CH_3 compounds but this situation is also vague, since the question of the extent of π-bonding to the aryl ligand remains open. Arnold and Bennett [29]

---

* Without the *o*-OCH_3 group, ${}^{1}J$(Pt, P) 1490 Hz, H. Motschi, PhD dissertation, ETH Zürich 1979.

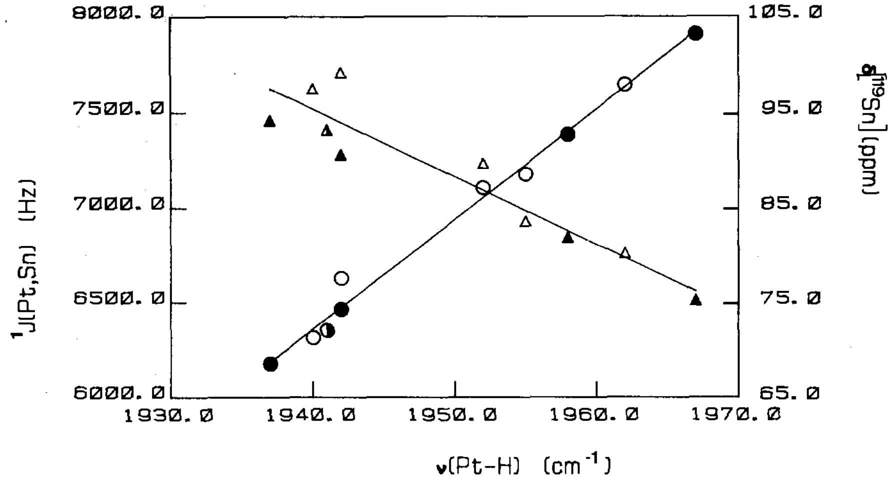

Fig. 5. Plots of ^1J(Pt, Sn), left ordinate, and $\delta(^{119}Sn)$, right ordinate, for the complexes *trans*-$[Pt(SnCl_3)(C_6H_4Y)(PEt_3)_2]$ vs. ν(Pt–H) for the complexes *trans*-$[PtH(C_6H_4Y)(PEt_3)_2]$. Circles refer to ^1J(Pt, Sn) and the triangles to $\delta(^{119}Sn)$ solid circles or triangles refer to *meta*-substituted complexes.

have made detailed ^1H, ^{31}P NMR and IR spectroscopic studies of the complexes *trans*-$[PtH(C_6H_4Y)(PEt_3)_2]$. From the ν(Pt–H) data: they conclude that the aryl ligands transmit their effects to the Pt–H bond by a predominantly inductive mechanism. A plot of our ^1J(Pt, Sn) values vs. ν(Pt–H) for these hydride complexes. Figure 5 gives a good linear correlation, and suggests that similar factors effect both physical parameters *. Since varying the *meta* substituent causes a larger change in ^1J(Pt, Sn), as noted above, we are inclined to agree with Arnold and Bennett but we note that in the plot involving ^1J(Pt, Sn) and ν(Pt–H) the largest deviation from linearity is for the *p*-OCH_3 complex. Given the sensitivity of ^1J(Pt, Sn) to inductive effects it is possible that the normally large resonance effect of the *p*-OCH_3 group is opposed by a significant inductive effect. This suggests that aryl–Pt π-bonding is present, but playing a secondary role. Further support for this comes from Fig. 5, where $\delta(^{119}Sn)$ is plotted against ν(Pt–H) for the hydrides and where the *p*-OCH_3 group again shows a marked deviation. In summary, there is no compelling NMR evidence for a large π-interaction between the metal and the aryl ligand but a small effect cannot be excluded.

(d) The molecular structure of trans-$[Pt(SnCl_3)(COPh)(PEt_3)_2]$

In view of the questions concerned with the benzoyl and $SnCl_3$ bonding in **1c** we have determined its molecular structure by X-ray diffraction. Suitable crystals of the complex *trans*-$[Pt(SnCl_3)(COPh)(PEt_3)_2]$ were obtained from CH_2Cl_2/Et_2O. An ORTEP plot of the molecule is shown in Fig. 6; the complex has slightly distorted square planar geometry at platinum with *trans*-PEt_3 ligands, and a summary of bond separations and bond angles is shown in Table 4.

The most interesting feature in the Table is the relatively long Pt-Sn bond separation, 2.634(1) Å (see Table 5 for data for comparison), since this represents the

---

* The small range for ^1J(Pt, H) and the large uncertainty reported [29] make this parameter unsuitable for comparison.

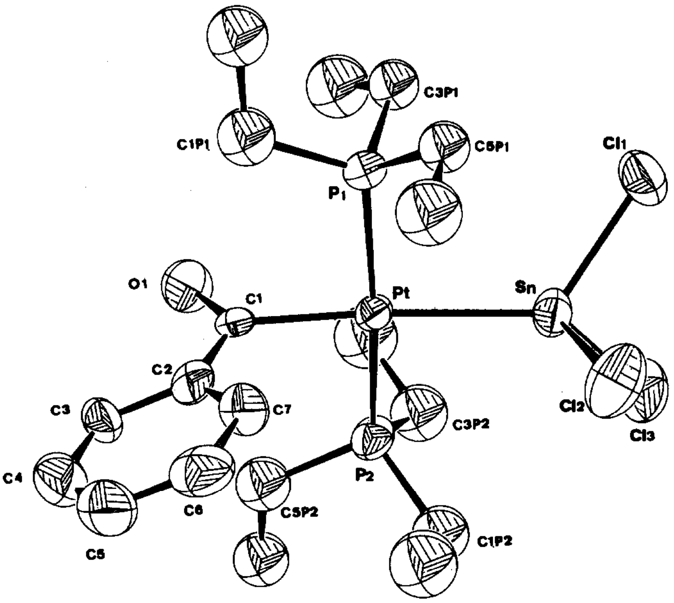

Fig. 6. ORTEP view of the molecule *trans*-[Pt($SnCl_3$)(COPh)(PEt_3)$_2$] (**1c**).

TABLE 4

SELECTED BOND DISTANCES (Å), BOND ANGLES (°) AND TORSION ANGLES (°) FOR **1c**

Pt-Sn	2.634(1)	Pt-Sn-Cl(1)	123.9(1)
Pt-P(1)	2.324(4)	Pt-Sn-Cl(2)	112.3(1)
Pt-P(2)	2.329(4)	Pt-Sn-Cl(3)	125.0(1)
Sn-Cl(1)	2.381(6)	Pt-C(1)-O	120.5(7)
Sn-Cl(2)	2.369(7)	Pt-C(1)-C(2)	117.4(9)
Sn-Cl(3)	2.398(6)	Cl(1)-Sn-Cl(2)	97.5(2)
Pt-C(1)	2.05(1)	Cl(1)-Sn-Cl(3)	94.9(2)
C(1)-O(1)	1.23(2)	Cl(2)-Sn-Cl(3)	97.2(2)
C(1)-C(2)	1.48(2)	C(2)-C(1)-O(1)	120.4(1.0)
C(2)-C(3)	1.40(2)	C(1)-C(2)-C(3)	121.5(1.1)
C(2)-C(7)	1.39(3)	C(1)-C(2)-C(7)	120.0(1.2)
C(3)-C(4)	1.36(3)	C(2)-C(3)-C(4)	121.6(1.4)
C(4)-C(5)	1.36(3)	C(2)-C(7)-C(6)	120.6(1.4)
C(5)-C(6)	1.38(4)	C(3)-C(4)-C(5)	120.3(1.7)
C(6)-C(7)	1.38(3)	C(3)-C(2)-C(7)	118.4(1.3)
		C(4)-C(5)-C(6)	123.0(1.6)
P-C [a]	1.82(2)	C(5)-C(6)-C(7)	115.7(1.7)
C-C [a]	1.49(6)		
		P-C-C [a]	115.6(2.2)
P(1)-Pt-P(2)	170.7(6)		
Sn-Pt-C(1)	173.0(3)	Sn-Pt-C(1)-C(2)	−6.8(1.8)
Sn-Pt-P(1)	92.1(1)	Sn-Pt-C(1)-O(1)	−179.0(2.0)
Sn-Pt-P(2)	91.7(1)	Pt-C(1)-C(2)-C(3)	−155.1(2.5)
P(1)-Pt-C(1)	88.8(4)	Cl(2)-Sn-Pt-C(1)	−6.9(2.0)
P(2)-Pt-C(1)	88.3(4)	C(3)-C(2)-C(1)-O(1)	16.5(3.0)

[a] Average value; e.s.d.'s calculated from the "scatterer" formula $s(x) = [(\Sigma_i(x_i - \bar{x})^2)/(N-1)]^{1/2}$.

TABLE 5

CRYSTALLOGRAPHIC DATA FOR $SnCl_3$ AND ACYL COMPLEXES

Compound	Pt–Sn (Å)	ref.
cis-$[PtCl_2(SnCl_3)_2]^{2-}$	2.355(8)	40
syn−*trans*-$[PtCl(SnCl_3)(PEt_3)]_2$	2.487(3)	4
$[PtCl(SnCl_3)(PhC(NH_2)=NOH)(PEt_3)]$	2.501(1)	45
$[PtCl(SnCl_3)(NH_2C_6H_4$-*p*-$Cl)(PEt_3)]$	2.514(1)	24
$[Pt(SnCl_3)_5]^{3-}$	2.553(7)	46
	2.572(10)	
$[PtCl(SnCl_3)(DIOP)]$	2.598	47
trans-$[Pt(SnCl_3)_2(P(OPh)_3)_2]$	2.599(2)	3a
$[Pt(SnCl_3)_3(AsMe_3)_2]^-$	2.602(2)	39
$[Pt(SnCl_3)_3(1,5\text{-}COD)]^-$	2.643(2)	36
	2.568(2)	
	2.546(2)	
trans-$[Pt(SnCl_3)(COPh)(PEt_3)_2]$	2.634(1)	this work
	M–CO (Å)	
$Pt(SnCl_3)(COPh)(PEt_3)_2$	2.05(1)	this work
$PCl(COPr^n)(PPh_3)_2$	2.002(19)	33
$PdCl(COPr^n)(PPh_3)_2$	1.996(6)	33
$PtCl(COHex^n)(PPh_3)_2$	2.02(1)	48
$PtCl(COCH_3)(PMePh_2)_2$	2.028(6)	49
$PtCl(COCF_3)(PMePh_2)_2$	1.960(4)	50
cis-$Pt(OC_6H_4CO)(PTol_3)_2$	1.96(2)	31
$[Pt(\mu\text{-}Cl)(COEt)(PMe_2Ph)]_2$	1.972(5)	50
$[PtCl_2(CONPr^i{}_2)(CO)]^-$	1.96(2)	37
$[PdCl\{COCH_2CH(R)NEt_2\}NHEt_2]$	1.96(2)	36

longest Pt–Sn separation observed in square planar platinum complexes. The only examples of longer M–Sn bonds are to be found in the five-coordinate complexes $[Ir(SnCl_3)(1,5\text{-}COD)_2]$ [38], 2.642(2) Å and $[Pt(SnCl_3)_3(1,5\text{-}COD)]^-$, [39], 2.643(2) Å, with the last value arising from the pseudo axial $SnCl_3{}^-$ in this distorted square pyramidal anion. The large bond separation in **1c** correlates nicely with the small ^1J(Pt, Sn) value described above, and supports the idea of a strong *trans* influence for the benzoyl ligand.

Including **1c**, the range of Pt–Sn bond separations is ca. 0.28 Å, and since we now have a qualitative view of the changes in both the Pt–Sn distance and ^1J(Pt, Sn) it is informative to plot these two parameters against one another and Fig. 7 shows such a plot for four-coordinate platinum(II) compounds. Despite the differing charges and ancillary ligands (each with its own *cis* effect) the general trend is clear. Interestingly, the Pt–Sn separation for the *cis*-$[PtCl_2(SnCl_3)_2]^{2-}$ anion [40] is sufficiently different from the remaining values as to cast doubt on the formulation of this complex as a straightforward $SnCl_3$ compound. Indeed, there is disorder in the crystal [40] such that one does not find discrete $SnCl_3$ ligands. Moreover, there is a suggestion of bridging character for the Sn and one Cl of the $SnCl_3$, and we believe these are responsible for the unusually short bond separation observed in this structure.

The benzoyl ligand is not quite planar (the dihedral angle C–C–C–O is 16.5°) and is situated such that the carbonyl C–O vector is almost perpendicular with

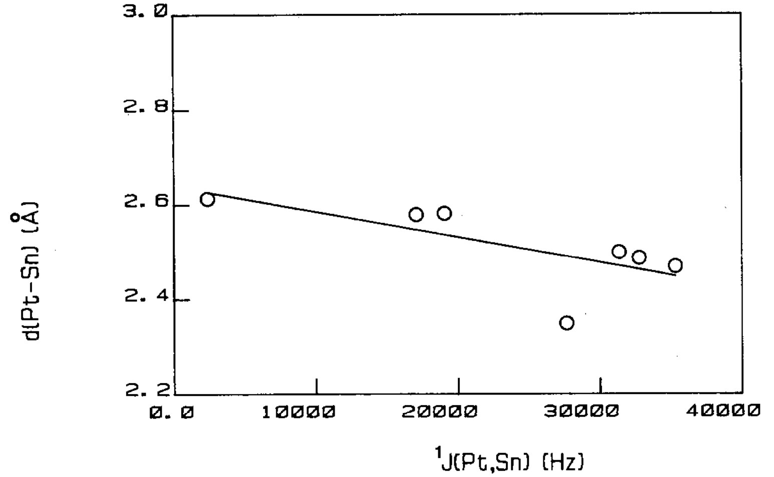

Fig. 7. Plot of the Pt–Sn separation (Å), vs. ^1J(Pt, Sn) (Hz), in some square planar $SnCl_3$ complexes of platinum.

respect to the coordination plane (the torsion angles P(1)–Pt–C–O and P(2)–Pt–C–O are 85 and −86°, respectively).

The Pt–C separation at 2.05(1) Å, although not significantly different from those found in other acyl-platinum and -palladium complexes (see Table 5), is at the high end of the observed range. For extensive acyl-platinum $p\pi$–$d\pi$ back bonding in **1c**, a relatively short Pt–C bond is to be expected. It is conceivable that the acyl ligand interacts strongly with metal d-π electrons in all the cases cited in Table 5 (the observed M–C separations are equal to, or shorter than, the sum of the covalent radii for Pt and carbonyl carbon, ca. 2.02 Å) but a more detailed analysis would require more accurate data than are currently available.

The platinum–phosphorus distances at 2.324(4) Å and 2.329(4) Å are typical for a *trans* geometric arrangement [14,34,41], and the bond distances and angles within the individual PEt_3 ligands are normal.

In conclusion, we feel confident that the benzoyl ligand has both a large structural and a large NMR *trans* influence, but the exact nature of the platinum–acyl bonding is still uncertain.

Experimental

NMR spectra were measured on a Bruker WM-250 MHz spectrometer, with samples in 10 mm tubes. Chemical shifts are relative to external H_3PO_4, Me_4Sn and Na_2PtCl_6 for ^{31}P, ^{119}Sn and ^{195}Pt, respectively. ^1H and ^{13}C data are referred to TMS. Solvents and temperature are shown in the footnotes to the Tables. The ^{31}P spectra were obtained using 35° pulses with a 0.6 s acquisition time, and the ^{119}Sn and ^{195}Pt spectra were collected using 60–65° pulses with 0.3 s acquisition times. Chemical shifts are correct to within ±0.1 ppm for ^{31}P and ±0.5 ppm for ^{119}Sn and ^{195}Pt nuclei. Coupling constants are correct to within ±2 Hz for ^{31}P and ±12 Hz for those derived from the ^{119}Sn and ^{195}Pt data.

The solvents were dried and degassed. $[Pt(PEt_3)_3]$ was prepared as previously described [51]. The benzoyl chloride and aryl bromides were obtained commercially and used without further purification. Typical preparative procedures for representative complexes are shown below.

trans-[PtBr(C_6H_5)(PEt_3)$_2$]. An orange colored solution of [Pt(PEt_3)$_3$] (0.35 g, 0.64 mmol) and bromobenzene (0.66 ml, 6.4 mmol) in toluene (5 ml) was heated under reflux for 2 h, during which the solution became yellow. Concentration under vacuum gave a yellow solid residue, which was recrystallized from EtOH; yield 0.227 g (61%). Found: C, 36.88; H, 5.97; Br, 12.70. $C_{18}H_{35}BrPPt$ calcd.: C, 37.74; H, 6.00; Br, 13.59%.

m-bis{trans-bromobis(triethylphosphine)platinum(II)}benzene. A solution of [Pt(PEt_3)$_3$] (1.018 g, 1.855 mmol) *m*-dibromobenzene (0.219 g, 0.928 mmol), and toluene (7 ml) was heated under reflux for 3 h. Removal of the solvent under vacuum gave a solid, which was recrystallized from EtOH to afford the colorless product; yield 0.740 g, (73%). Found: C, 32.99; H, 5.93; Br, 15.53%. $C_{30}H_{64}Br_2P_4Pt_2$ C, 32.80; H, 5.87; Br, 14.55%.

trans-[Pt($SnCl_3$)(C_6H_5)(PEt_3)$_2$]. A solution of *trans*-[PtBr(C_6H_5)(PEt_3)$_2$] (0.113 g, 0.193 mmol) in MeOH (10 ml) was treated with a solution of $AgBF_4$ (0.0377 g, 0.193 mmol) in MeOH (5 ml). The AgBr was filtered off and LiCl (0.0081 g, 0.193 mmol) was added. Evaporation under vacuum was followed by extraction of the residual chloro complex into toluene. Removal of the toluene was followed by addition of 10 ml CH_2Cl_2 and $SnCl_2$ (0.11 g, 0.58 mmol) and after 2 h stirring at room temperature the excess $SnCl_2$ was removed by filtration. Removal of the CH_2Cl_2 solvent gave the product, yield 0.115 g (74%). Found: C, 29.54; H, 4.84; Cl, 14.77. $C_{18}H_{35}Cl_3P_2PtSn$ calcd.: C, 29.46; H, 4.81; Cl, 14.50%.

m-Bis{trans-trichlorostannatobis(triethylphosphine)platinum(II)}benzene. A solution of [C_6H_4-*m*-{PtBr(PEt_3)$_2$}$_2$] (0.109 g, 0.0988 mmol) in MeOH (10 ml) was treated with one of $AgBF_4$ (0.0385, 0.198 mmol) in MeOH (5 ml). The AgBr was filtered off and LiCl (0.0084 g, 0.198 mmol) was added. Evaporation left the chloro complex, which was extracted into toluene. After removal of the toluene in vacuum and addition of 10 ml of CH_2Cl_2 and $SnCl_2$ (0.112 g, 0.593 mmol) the suspension was stirred at room temperature for 2 h. The excess of $SnCl_2$ was filtered off, and evaporation of the CH_2Cl_2 solution gave the product. Yield 0.069 (50%). Found: C, 26.78; H, 4.69; Cl, 14.91. $C_{30}H_{64}Cl_6P_4Pt_2Sn_2$ calcd.: C, 25.94; H, 4.64; Cl, 15.31%.

trans-[Pt($SnCl_3$)(C_6H_4-m-CF_3)(PEt_3)$_2$]. A solution of *trans*-[PtCl(C_6H_4-*m*-CF_3)(PEt_3)$_2$] (0.079 g, 0.13 mmol) in CH_2Cl_2 (3 ml) was treated with tin(II) chloride (0.025 g, 0.13 mmol), and the resulting suspension stirred until all the $SnCl_2$ had dissolved (ca. 0.5 h). Filtration of the solution was followed by removal of the CH_2Cl_2 and drying of the residue under vacuum. Yield 0.070 g (68%). Found: C, 28.39; H, 4.28; Cl, 13.60%. $C_{19}H_{34}Cl_3F_3PtP_2Sn$ calcd.: C, 28.47, 4.28; Cl, 13.27%.

The complex *trans*-[Pt($SnCl_3$)(C_6H_4-*m*-OCH_3)(PEt_3)$_2$] was prepared in the same way. Yield 0.031 g (59%). Found: C, 30.14; H, 5.01; Cl, 13.91. $C_{19}H_{37}Cl_3OP_2PtSn$ calcd.: C, 29.89; H, 4.88; Cl, 13.93%.

trans-[Pt($SnCl_3$)(COC_6H_5)(PEt_3)$_2$]. A solution of benzoyl chloride (2.2 g, 15.4 mmol) in toluene (20 ml) was added dropwise to a solution of [Pt(PEt_3)$_3$] (2.0 g, 4.8 mmol) in 20 ml toluene. Stirring for 24 h at room temperature followed by removal of the toluene under vacuum left the crude chloro complex, yield 1.13 g (74%). (The microanalysis of this complex was satisfactory.) This product (254 mg, 0.443 mmol) was dissolved in CH_2Cl_2 (3 ml) and the solution was treated with solid $SnCl_2$ (48.1

TABLE 6

CRYSTALLOGRAPHIC DATA COLLECTION FOR **1c**

Formula	$PtSnCl_3P_2OC_{19}H_{35}$
Mol. wt.	761.575
Crystal dimensions (mm)	0.35 × 0.15 × 0.07
Crystal system	orthorhombic
Space group	$P2_12_12_1$
a (Å)	10.266(3)
b (Å)	15.476(2)
c (Å)	17.440(2)
Z	4
V (Å^3)	2770.8
ρ (calc., g cm^{-3})	1.868
μ (cm^{-1})	64.5
Radiation	Mo-$K_{\bar{\alpha}}$ (λ 0.71069 Å)
Measured reflections	$+h$ $+k$ $+l$
2θ range (deg)	2.6–25.0
Scan type	$\omega/2\theta$
max. scan speed (deg. min^{-1})	10.5
max. counting time (sec)	60
Scan width (deg)	$1.0 + 0.35 \tan\theta$
Background time	0.5 × scan time
Receiving aperture	$1.85 + \tan\theta$ (hor.)
	4.0 mm (vert.)
Prescan rejection limit	0.5 (2σ)
Prescan acceptance limit	0.03 (33σ)
No. of independent data (obs. data)	2733 (2303)
R^a (obs. reflection)	0.035
$R_w{}^b$	0.043

[a] $R = \Sigma(|F_0| - |F_c|)/\Sigma|F_0|$. [b] $R_w = [\Sigma w(|F_0| - |F_c|)^2/\Sigma w F_0{}^2]^{1/2}$.

mg, 0.443 mmol). Stirring for 10 min at room temperature was followed by filtration, and a layer of Et_2O (ca. 9 ml) was introduced above the CH_2Cl_2. After two weeks at −20°C the yellow crystals were filtered off. Yield 0.220 g (65%). Found: C, 29.47; H, 4.85; Cl, 13.27. $C_{19}H_{35}Cl_3OP_2PtSn$ calcd.: C, 29.96; H, 4.63; Cl, 13.97%.

Suitable crystals for X-ray diffraction were obtained by slow evaporation from a CH_2Cl_2/Et_2O solution and were air stable. Cell constants were obtained by least squares fit of the 2θ values of 25 high-angles reflections ($11.0 \leqslant \theta \leqslant 15.0$) using the centering routines of the Enraf–Nonius CAD4/SDP diffractometer [42]. Crystallographic data and details of the data collection are given in Table 6. Data were collected with variable scan speed to give a constant statistical precision of the collected intensities. Three standard reflections, measured every hour, were used to check the stability of the crystal and of the experimental conditions, and no significant variation was detected. The orientation of the crystal was checked every 300 reflections. Data were corrected for Lorentz and polarization effects, and for absorption using the azimuthal ψ scans of 6 reflections at increasing θ values: 301, 401, 501, 702, 812, 902, using the data reduction programs of the CAD4/SDP package [42]. Transmission factors were in the range 0.89–0.99. Intensities were considered as observed if $F_0 \geqslant 3\sigma(F_0)$, while a value of F_0 of 0.0 was given to reflections with negative observed intensities. The structure was solved by a com-

TABLE 7

FINAL POSITIONAL PARAMETERS FOR $[Pt(SnCl_3)(CoPh)(PEt_3)_2]$. (E.s.d.'s are given in parentheses)

Atom	*x/a*	*y/b*	*z/c*
Pt	0.18333(5)	−0.05009(3)	−0.12033(3)
Sn	0.41275(10)	0.02552(7)	−0.11225(7)
Cl(1)	0.59755(52)	−0.03629(38)	−0.05065(39)
Cl(2)	0.50809(72)	0.04562(47)	−0.23463(36)
Cl(3)	0.45041(59)	0.16868(34)	−0.06444(37)
P(1)	0.27564(42)	−0.18699(25)	−0.11386(27)
P(2)	0.07582(44)	0.08171(26)	−0.10781(31)
C(1)	0.00652(143)	−0.10676(95)	−0.14074(100)
C(2)	−0.04105(172)	−0.10759(91)	−0.22068(101)
C(3)	−0.17468(175)	−0.11529(116)	−0.23585(107)
C(4)	−0.22360(219)	−0.11390(156)	−0.30817(138)
C(5)	−0.13977(250)	−0.10454(153)	−0.36782(129)
C(6)	−0.00687(256)	−0.09687(129)	−0.35705(118)
C(7)	0.04213(207)	−0.09719(121)	−0.28310(101)
O(1)	−0.06156(124)	−0.13254(91)	−0.08702(77)
C(1P1)	0.16659(224)	−0.27549(143)	−0.13952(123)
C(2P1)	0.22345(249)	−0.36678(154)	−0.13245(133)
C(3P1)	0.32128(199)	−0.20624(118)	−0.01431(103)
C(5P1)	0.42274(186)	−0.20606(117)	−0.16758(101)
C(1P2)	0.12927(238)	0.16464(151)	−0.17574(132)
C(3P2)	0.09916(255)	0.12636(163)	−0.01339(138)
C(5P2)	−0.10027(212)	0.08002(136)	−0.11809(128)

bined use of Patterson and Fourier methods and refined by block-diagonal least squares using anisotropic temperature factors for Pt, Sn, P, O atoms and for the carbons of the benzaldehyde moiety, and isotropic factors for the other. During the last stage of the refinement the hydrogen atoms were introduced in their calculated positions (assuming a C–H separation of 0.95 Å) but not refined. The real and imaginary parts of the anomalous scattering were taken into account [43]; scattering factors were taken from ref. 43. A Cruickshank weighting scheme was used throughout the refinement [44]. Final atomic coordinates are listed in Table 7. A list of thermal parameters, calculated hydrogen positions and a Table of F_{obs}/F_{calc} may be obtained from the authors upon request.

Acknowledgements

We thank the Swiss National Science Foundation for support for H.J.R., the Italian C.N.R. and the Johnson Matthey Research Center, England, for the loan of platinum metals.

References

1 (a) L.M. Venanzi, Pure Appl. Chem., 52 (1980) 1117; (b) P.S. Pregosin and R.W. Kunz, NMR Basic Principles and Progress, Springer Verlag, 1979, vol. 16.

2 R.K. Harris and B.E. Mann, NMR and the Periodic Table, Academic Press, London, New York, 1978.

3 (a) A. Albinati, P.S. Pregosin and H. Rüegger, Inorg. Chem., 23 (1984) 3223; (b) idem, Angew. Chem. Int. Ed. Engl., 23 (1984) 78; (c) K.H.A. Ostoja Starzewski, P.S. Pregosin and H. Rüegger, Helv. Chim. Acta, 65 (1982) 785.

4 A. Albinati, R. Naegeli, K.H.A. Ostoja Starzewski, P.S. Pregosin and H. Rüegger, Inorg. Chim. Acta, 76 (1983) L231.

5 M. Kretschmer, P.S. Pregosin and H. Rüegger, J. Organomet. Chem., 241 (1983) 87.

6 M. Kubota, D.A. Phillips and J.E. Jacobsen, J. Coord. Chem., 10 (1980) 125.

7 B.E. Mann and B.F. Taylor in ^{13}C NMR Data for Organometallic Compounds, Academic Press, London, New York, 1981.

8 P.S. Pregosin and H. Rüegger, Inorg. Chim. Acta, 86 (1984) 55.

9 (a) J.F. Nixon and A. Pidcock, Ann. Rev. NMR Spectrosc., Academic Press, London, New York, 1969, vol. 2, p. 345; (b) J.P. Jesson, in E. Muetterties (Ed.), Transition Metal Hydrides, Marcel Dekker, New York, 1971, and ref. therein.

10 K.H.A. Ostoja Starzewski and P.S. Pregosin, in E.C. Alyea and D.W. Meek (Eds.), Catalytic Aspects of Metal Phosphine Complexes, Advances in Chemistry Series, Washington, 1982, vol. 196, p. 23.

11 H. Rüegger, PhD Dissertation Nr. 7402 ETH Zürich, 1983.

12 P.S. Pregosin, Coord. Chem. Rev., 44 (1982) 247.

13 G. Butler, C. Eaborn and A. Pidcock, J. Organomet. Chem., 181 (1979) 47.

14 P.S. Pregosin, R. Favez, R. Roulet, T. Boschi and R.A. Michelin, Inorg. Chim. Acta, 45 (1980) L7.

15 (a) J.A. Pople and D.P. Santry, Mol. Phys., 8 (1964) 1; (b) 9 (1965) 311.

16 N.F. Ramsay, Phys. Rev., 78 (1950) 699.

17 (a) L.M. Venanzi, Chem. Brit., 4 (1968) 162; (b) A. Pidcock, R. Richards and L.M. Venanzi, J. Chem. Soc. A, (1966) 1707.

18 (a) T.G. Appleton, H.C. Clark and L.E. Manzer, Coord. Chem. Rev., 10 (1973) 335; (b) G.K. Anderson, H.C. Clark and J.A. Davies, Inorg. Chem., 20 (1981) 1636; (c) H.C. Clark and L.E. Manzer, ibid., 11 (1972) 2749.

19 F.H. Allen, A. Pidcock and C.R. Waterhouse, J. Chem. Soc. A, (1970) 2087.

20 (a) J. Powell and B.L. Shaw, J. Chem. Soc., (1965) 3879; (b) J. Chatt and B.L. Shaw, ibid., (1962) 5075; (c) M.J. Church and N.J. Mays, J. Chem. Soc. A, (1968) 3074.

21 G.G. Mather, G.J.N. Rapsey and A. Pidcock, Inorg. Nucl. Chem. Lett., 9 (1973) 567.

22 M.H. Chisholm, H.C. Clark, L.E. Manzer, J.B. Stothers and J.E.H. Ward, J. Am. Chem. Soc., 95 (1973) 8574.

23 (a) H. Motschi, P.S. Pregosin and L.M. Venanzi, Helv. Chim. Acta, 62 (1979) 667; (b) P.S. Pregosin, H. Omura and L.M. Venanzi, J. Am. Chem. Soc., 95 (1973) 2047.

24 A. Albinati, H. Moriyama, H. Rüegger, P.S. Pregosin and A. Togni, Inorg. Chem., in press.

25 M.A. Cairns, K.R. Dixon and G.A. Rivett, J. Organomet. Chem., 171 (1979) 373.

26 D. Carmona, S. Chaloupka, J. Jans, R. Thouvenot and L.M. Venanzi, J. Organomet. Chem., 275 (1984) 303.

27 C. Crocker, R.J. Goodfellow, J. Gimeno and R. Usón, J. Chem. Soc. Dalton Trans., (1977) 1448.

28 P.S. Pregosin and S.N. Sze, Helv. Chim. Acta, 61 (1978) 1848.

29 D.P. Arnold and M.A. Bennett, Inorg. Chem., 23 (1984) 2117.

30 (a) D.P. Arnold and M.A. Bennett, J. Organomet. Chem., 199 (1980) C17; (b) idem, Inorg. Chem., 23 (1984) 2110.

31 C.G. Anklin, P.S. Pregosin, F. Bachechi, P. Mura and L. Zambonelli, J. Organomet. Chem., 222 (1981) 175.

32 T.G. Appleton and M.A. Bennett, Inorg. Chem., 17 (1978) 738.

33 R. Bardi, A.M. Piazzesi, C. Cavinato, P. Cavoli and L. Toniolo, J. Organomet. Chem., 224 (1982) 407.

34 W. Conzelmann, J.D. Koola, U. Kunze and J. Strahle, Inorg. Chim. Acta, 89 (1984) 147.

35 (a) C.G. Anklin and P.S. Pregosin, J. Organomet. Chem., 243 (1983) 101; (b) H. Motschi, P.S. Pregosin and H. Rüegger, ibid., 193 (1980) 397.

36 L. Hegedus, O.P. Anderson, K. Zetterberg, G. Allen, K. Sürola-Hansen, D.J. Olsen and A.B. Packard, Inorg. Chem., 16 (1977) 1887.

37 D.B. Dell'Amico, F. Calderazzo and G. Pelizzi, Inorg. Chem., 18 (1979) 1165.

38 P. Porta, M.H. Powell, R.J. Mowby and L.M. Venanzi, J. Chem. Soc. A, (1967) 455.

39 P.S. Pregosin, H. Rüegger, A. Albinati and R. Naegeli, Angew. Chem., 94 (1982) 310.

40 N.W. Alcock and J.H. Nelson, J. Chem. Soc. Dalton Trans., (1982) 2415.

41 S. Krogsrud and J.A. Ibers, Inorg. Chem., 14 (1975) 2298.

42 Enraf–Nonius Structure Determination Package (SDP): Enraf–Nonius, Delft, Holland, 1980.

43 International Tables for X-ray Crystallography, vol. IV, Birmingham, The Kynoch Press.

44 D.W.J. Cruickshank in A. Ahmed (Ed.), Computing Methods in Crystallography, Munksgaard, Copenhagen, 1972.

45 A. Goel, S. Goel and D. Vanderveer, Inorg. Chim. Acta, 54 (1981) L5.

46 N.W. Alcock and J.H. Nelson, Inorg. Chem., 21 (1982) 1196.

47 G. Consiglio, P. Pino and M. Scallone, unpublished results.

48 R. Bardi, A.M. Piazzesi, A. DelPra, G. Cavinato and L. Toniolo, J. Organomet. Chem., 234 (1982) 107.

49 M.A. Bennett, K.C. Ho, J.C. Jeffery, G.M. McLaughlin and G.B. Robertson, Aust. J. Chem., 35 (1982) 1311.

50 G.K. Anderson, R.J. Cross, L.M. Muir, K.W. Muir and J. Solamun, J. Organomet. Chem., 170 (1979) 385.

51 T. Yoshida, T. Matsuda and S. Otsuka, Inorg. Synth., 19 (1979) 110.